0026-895X/97/061131-06$3.00/0

MOLECULAR PHARMACOLOGY, **52:**1131–1136 (1997).

KvLQT1 Potassium Channel but Not IsK Is the Molecular Target for *trans*-6-Cyano-4-(*N*-ethylsulfonyl-*N*-methylamino)-3-hydroxy-2,2-dimethyl-chromane

GILDAS LOUSSOUARN, FLAVIEN CHARPENTIER, RAHA MOHAMMAD-PANAH, KARL KUNZELMANN, ISABELLE BARÓ and DENIS ESCANDE

Laboratoire de Physiopathologie et de Pharmacologie Cellulaires et Moléculaires, Institut National de la Santé et de la Recherche Médicale CJF96–01, Hôpital Hotel-Dieu, Nantes, France (G.L., F.C., R.M-P, I.B., D.E.), and Institute of Physiology, Albert-Ludwigs-Universität, Freiburg, Germany (K.K.)

Received June 13, 1997; Accepted August 29, 1997

SUMMARY

Mutations in the *KvLQT1* gene are the cause for the long QT syndrome [*Circulation* **94:**1996–2012 (1996)]. Coexpression of KvLQT1 in association with the channel regulator protein IsK produces a K^+ current with characteristics reminiscent of the slow component of the delayed rectifier in cardiac myocytes. We explored the pharmacological properties of *trans*-6-cyano-4-(*N*-ethylsulfonyl-*N*-methylamino)-3-hydroxy-2,2-dimethyl-chromane (293B), a chromanol compound, on the K^+ current produced by direct intranuclear injection of KvLQT1 and IsK cDNA plasmids in COS-7 cells. Injected cells were recorded by means of the whole-cell and cell-attached patch-clamp configurations under chloride-free conditions. Cells injected with KvLQT1 cDNA alone exhibited a fast-activating outward K^+ current, whereas cells coinjected with KvLQT1 plus IsK cDNAs exhibited a time-dependent outward current with slower activation kinetics. The chromanol 293B blocked the K^+ current related to KvLQT1 expression in both the absence or presence of IsK. The IC_{50} value for 293B to block KvLQT1-related current was not significantly modified by the presence of IsK (9.9 μM in the absence of IsK versus 9.8 μM in its presence). The block produced by 293B was strongly voltage-dependent inasmuch as it was close to 0 at −80 mV and occurred during a depolarizing voltage step. The time constants for the drug to block the current were in the same order of magnitude as activation kinetics of the current. Kinetics for drug unblock at the holding potential were much faster, in the order of a few tenths of a msec. KvLQT1 currents recorded in the cell-attached configuration were also blocked by externally applied 293B, suggesting that the compound penetrated the cell to block the channel. Cromakalim, another chromanol compound, also blocked KvLQT1 currents. Our results show that the chromanol compound 293B is targeted to KvLQT1 channels but not to the IsK regulator.

Mutations in the *KvLQT1* gene have been recognized as the most frequent cause for the autosomal dominant (Romano-Ward) form of the long QT syndrome, a life-threatening familial disorder characterized by prolonged cardiac repolarization (1). *KvLQT1* was also demonstrated to be responsible for the recessively inherited Jervell and Lange-Nielsen cardioauditory syndrome characterized by a bilateral deafness associated with prolonged cardiac repolarization (2). Finally, the *KvLQT1* gene, which comprises 14 exons and spans a large 300-kilobase pair genomic region at chromosomal region 11p15.5, encompasses chromosomal rearrangements associated with the Beckwith-Wiedemann syndrome, which causes prenatal overgrowth and cancer but no cardiac repolarization anomalies (3). Within the past year, these successive discoveries enlightened the medical importance of *KvLQT1*, which may be implicated in at least three distinct genetic disease entities.

The *KvLQT1* gene product was very recently demonstrated to be a voltage-dependent K^+ channel with electrophysiological characteristics that are consistently modified by the presence of a membranous regulator protein termed IsK (4, 5). The *IsK* (also termed minK) gene product, which contains a single transmembrane domain, often was suspected to be itself a K^+ channel (6). This assumption was derived from the observation that injection of *Xenopus laevis* oocytes with IsK mRNA alone produced a voltage-dependent K^+ current (6–8). However, in 1993, Attali *et al.* (9) proposed that IsK acts as a channel regulator but not as a channel protein. In agreement with this latter interpretation, transfection of

This work was supported by grants from the Association Française de Lutte contre la Mucoviscidose and the Institut National de la Santé et de la Recherche Médicale. G.L. is recipient of a special grant from the Crédit Mutuel.

ABBREVIATIONS: 293B, *trans*-6-cyano-4-(*N*-ethylsulfonyl-*N*-methylamino)-3-hydroxy-2,2-dimethyl-chromane; HEPES, 4-(2-hydroxyethyl)-1-piperazineethanesulfonic acid; EGTA, ethylene glycol bis(β-aminoethyl ether)-*N*,*N*,*N*′,*N*′-tetraacetic acid; τ_{deact}, deactivation time constant; $\tau_{act\text{-}fast}$, fast time constant; $\tau_{act\text{-}slow}$, slow time constant.

mammalian cells with IsK cDNA produced no K^+ current (10). Discrepant results obtained in different expression systems were later explained by Sanguinetti *et al.* (5), who demonstrated that *X. laevis* oocytes constitutively express a KvLQT1 transcript that generates a K^+ current in the presence of IsK. In mammalian cells, expression of KvLQT1 alone but not of IsK alone produces a voltage-dependent K^+ current of small amplitude and fast activation kinetics. Coexpression of KvLQT1 plus IsK is associated with a K^+ current with physiological characteristics reminiscent of that of the endogenous i_{Ks} current, a major component of the delayed-rectifier sustained K^+ current in cardiac myocytes (11). Expression of KvLQT1 is not limited to the heart muscle and is also found in human pancreas, lung, kidney, and placenta (4, 5).

The medical importance of KvLQT1 prompted us to identify a pharmacological blocker that can be used as a tool to elucidate the physiological role of KvLQT1 K^+ channels in various organs. The chromanol compound 293B was a good candidate because it was previously found to block the K^+ current induced by expression of IsK in *X. laevis* oocytes (12). Here, we demonstrate that 293B is a potent blocker of human KvLQT1 K^+ channels and that it binds to the channel protein itself but not to the IsK regulator.

Materials and Methods

Intranuclear injection of plasmids. The African green monkey kidney-derived cell line COS-7 was obtained from the American Type Culture Collection (Rockville, MD) and cultured in Dulbecco's modified Eagle's medium supplemented with 10% fetal calf serum and antibiotics (100 IU/ml penicillin and 100 μg/ml streptomycin; all from GIBCO, Paisley, Scotland) at 37° in a humidified incubator. They were subcultured regularly by enzymatic treatment. Cells growth onto plastic Petri dishes with a glass coverslip bottom (Nunclon; InterMed Nunc, Roskilde, Denmark) were microinjected with plasmids at day 1 after plating. Our protocol to microinject cultured cells using the Eppendorf ECET microinjector 5246 system has been reported in detail previously (13). Plasmids were diluted at a final concentration of 5–50 μg/ml in a buffer of 50 mM HEPES, 50 mM NaOH, and 40 mM NaCl, pH 7.4, supplemented with 0.5% fluorescein isothiocyanate-dextran. The human KvLQT1 and IsK cDNAs (a kind gift from J. Barhanin, Sophia-Antipolis, France) were subcloned into the mammalian expression vector, pCI and pCR, respectively (Promega, Madison, WI) under the control of a cytomegalovirus enhancer/promoter (4).

Patch-clamp recordings. Whole-cell currents were recorded as described previously (13). A Petri dish containing cells was placed on the stage of an inverted microscope and superfused continuously with the standard extracellular solution. Patch pipettes with a tip resistance of 2.5–5 MΩ were electrically connected to a patch-clamp amplifier (Axopatch 200A; Axon Instruments, Foster City, CA). Stimulation, data recording, and analysis were performed with a software designed by Gérard Sadoc (DIPSI Industrie, Asnière, France) through an A/D converter (Tecmar TM100 Labmaster; Scientific Solution, Solon, OH). A microperfusion system allowed local application and rapid change of the different experimental solutions warmed at 35°. Patch-clamp measurements are presented as the mean ± standard error of the mean. Statistical significance of the observed effects was assessed by means of the Student's *t* test.

Solutions and drugs. The standard extracellular medium contained 145 mM NaCl, 4 mM KCl, 1 mM $MgCl_2$, 1 mM $CaCl_2$, 5 mM HEPES, and 5 mM glucose, pH adjusted to 7.4 with NaOH. For whole-cell patch-clamp recordings, the intracellular medium contained 145 mM K-gluconate, 5 mM HEPES, 2 mM EGTA, 2 mM $Mg_{½}$-gluconate (0.1 mM free Mg^{2+}), and 2 mM K_2ATP, pH 7.2 with KOH, and the extracellular medium contained 145 mM Na-gluconate, 4 mM K-gluconate, 7 mM $Ca_{½}$-gluconate (1 mM free Ca^{2+}), 4 mM $Mg_{½}$-gluconate (1 mM free Mg^{2+}), 5 mM HEPES, and 5 mM glucose, pH 7.4 with NaOH. For cell-attached recordings, the bath solution contained 145 mM K-gluconate, 4 mM $Mg_{½}$-gluconate 4 (1 mM free Mg^{2+}), 7 mM $Ca_{½}$-gluconate (1 mM free Ca^{2+}), and 5 mM HEPES, pH 7.2 with KOH, and the pipette solution contained 145 mM Na-gluconate, 4 mM K-gluconate, 7 mM $Ca_{½}$-gluconate (1 mM free Ca^{2+}), 4 mM $Mg_{½}$-gluconate (1 mM free Mg^{2+}), and 5 mM HEPES, pH 7.4 with NaOH. Compound 293B [*trans*-6-cyano-4-(*N*-ethylsulfonyl-*N*-methylamino)-3-hydroxy-2,2-dimethyl-chromane] was dissolved in dimethylsulfoxide so the final concentration of the solvent was <1. Cromakalim (Sigma Chemical) was dissolved in dimethylsulfoxide.

Results

KvLQT1 expression in COS-7 cells. Noninjected COS-7 cells or cells injected with the pCI plasmid alone exhibited no time-dependent current. Fig. 1 illustrates typical whole-cell recordings in COS-7 cells injected with KvLQT1 cDNA in the absence (Fig. 1A) and presence (Fig. 1B) of IsK. Cells injected with KvLQT1 plus IsK cDNAs exhibited a time-dependent outward current with a comparable amplitude but with slower activation kinetics than cells expressing KvLQT1 alone. Deac-

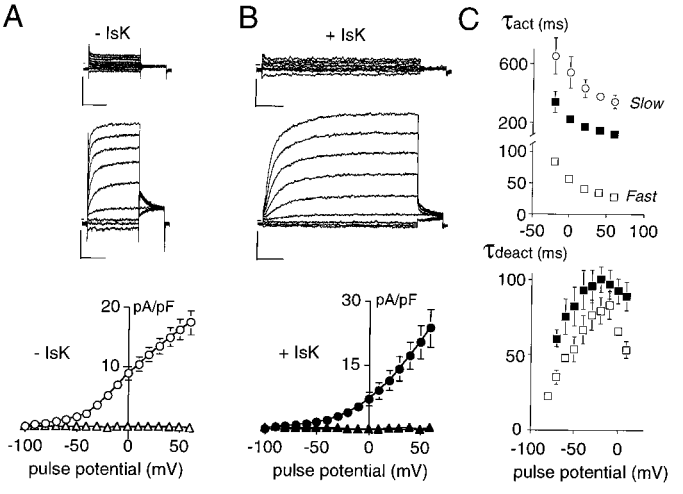

Fig. 1. KvLQT1-related K^+ currents in COS-7 cells in the absence and presence of the IsK regulator. A and B, *Top*, superimposed current *tracings* recorded in a noninjected control COS-7 cell (A) and a cell injected with 5 μg/ml pCR-IsK alone (B). *Middle*, current *tracings* in a cell injected with 5 μg/ml pCI-KvLQT1 without (A) and with (B) 5 μg/ml pCR-IsK. The voltage potential was stepped, in 10-mV increments, to various voltages (pulse potential) between −100 and +60 mV (for clarity, current traces are shown recorded in response to voltage steps of 20-mV increments) and then stepped back to −40 mV, where tail currents are visible. Holding potential, −80 mV. *Vertical bars*, 2.5 pA/pF. *Horizontal bars*, 500 msec. *Bottom*, current-voltage relationships for the time-dependent current activated by depolarization. A, Averaged data from noninjected cells (△) and cells injected with pCI-KvLQT1 alone (○) (five cells). B, Averaged data from cells injected with pCR-IsK alone (▲) and cells injected with pCR-IsK plus pCI-KvLQT1 (●) (six cells). C, Activation and deactivation time constants for the KvLQT1 current in relation to pulse potential. Values are mean ± standard error. *Top*, Activation time constants $\tau_{act\text{-}fast}$ (□) and $\tau_{act\text{-}slow}$ (○) for the rapid and slow components of the KvLQT1 current recorded in the absence of IsK (n = 9). ■, Activation time constant τ_{act} for the KvLQT1 current recorded in the presence of IsK (four cells). Same voltage protocol as in A and B. *Bottom*, deactivation time constants τ_{deact} for the KvLQT1 current in relation to pulse potential in the absence (□; four cells) and presence (■; four cells) of IsK. The voltage potential was stepped to +60 mV and then stepped back to various voltages between −100 and +60 mV, where tail-current τ_{deact} were measured.

tivating tail currents at −40 mV were fitted by a monoexponential decay that was extrapolated to time 0 to reliably measure tail current amplitude in the absence of contamination by the capacitative current. Under our experimental conditions, the current tail density so measured in cells injected with KvLQT1 cDNA alone (5.91 ± 1.08 pA/pF; prepulse potential to +40 mV; 15 cells) was not significantly different from that recorded in the presence of the IsK regulator (4.19 ± 0.64 pA/pF; 16 cells; $p > 0.5$). As observed previously by others (4), the activation threshold for the time-dependent current related to KvLQT1 expression was comparable in the presence and absence of IsK. In contrast, in cells coinjected with KvLQT1 plus IsK cDNAs, the potential for half-maximal activation ($V_{0.5}$ = 14.1 mV), was shifted in comparison with cells injected with KvLQT1 cDNA alone ($V_{0.5}$ = −23.2 mV). Fig. 1C illustrates activation and deactivation kinetics for KvLQT1. In cells expressing KvLQT1 alone, activation was adequately fitted by the sum of two exponential functions. Both $\tau_{act\text{-}fast}$ (which represented 83% of the total current) and $\tau_{act\text{-}slow}$ (which represented 17% of the total current) decreased at more depolarized voltages. In cells coexpressing KvLQT1 and IsK, activation kinetics were convincingly fitted by a single exponential with a time constant (τ_{act}) 10-fold greater than the activation time constant ($\tau_{act\text{-}fast}$) of the major component in cells expressing KvLQT1 alone. In contrast, as reported previously (13), deactivation time constants (τ_{deact}) were of the same order of magnitude in the presence and absence of IsK (Fig. 1C).

293B dose-dependently blocks KvLQT1-related K^+ current. We then tested the effects of 293B on the K^+ current related to KvLQT1 expression. In a concentration range of 0.1–100 μM, 293B dose-dependently blocked KvLQT1 tail currents. The dose-effect relations shown in Fig. 2A were obtained by measuring the tail current density at −40 mV in the presence of various concentrations of the drug. Exponential fits forced to time 0 were used to achieve this measurement. Fig. 2A shows that 293B blocked KvLQT1 currents regardless of the presence of IsK. The half-maximum concentration (IC_{50}) values for 293B to block tail currents related to KvLQT1 expression were 9.8 and 9.9 μM in the presence and absence of IsK, respectively. The blocking effects of 293B were fully reversible when the drug was washed off. The current blocked by 10 μM 293B obtained by digital subtraction and its current-voltage relationship are depicted in Fig. 2, B and C.

Voltage- and time-dependence of the block produced by 293B. KvLQT1 tail current-voltage relationships in a cell injected with KvLQT1 cDNA alone and recorded in the absence and presence of 10 μM 293B are superimposed in Fig. 3A. These curves suggested that the block produced by 293B was voltage-dependent in that for activation voltages of <−30 mV, the tail current amplitude in the presence of 293B was comparable in size to that recorded in control conditions. Averaged data (Fig. 3B) further substantiated the voltage-dependent effects of 293B. This curve was obtained by plotting the percentage of block produced by 293B at a concentration close to its IC_{50} (i.e., the current tail amplitude in the presence of 10 μM 293B subtracted from the current amplitude in control and divided by the tail current amplitude in control) for various prepulse potentials. Obviously, the amount of KvLQT1 block produced by 293B increased as the activation prepulse was set more positive. To further investigate the voltage-dependency of the block produced by 293B,

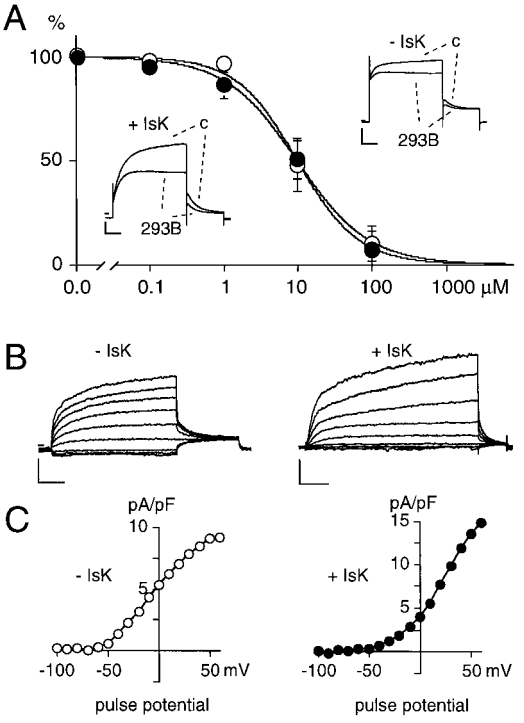

Fig. 2. The chromanol compound 293B blocks KvLQT1 currents. A, Dose-effect relationships for 293B to block KvLQT1 current in the absence (○) and presence (●) of IsK. The protocol consisted of depolarizing voltage steps applied from −80 to +40 mV and then back to −40 mV. *Data points* represent the normalized current tail amplitudes measured in the presence of various concentrations of 293B. *Data points*, mean ± standard error of four to seven experiments. Semilogarithmic plot in which data were fitted to a Hill equation, with a half-activation point at 9.9 μM (−IsK) and 9.8 μM (+IsK) and a steepness of 1.1 (−IsK) and 0.9 (+IsK). *Inset*, superimposed current traces recorded in control (C) and in the presence of 10 μM 293B in the presence (*left*; +IsK) and absence (*right*; −IsK) of IsK. *Vertical bars*, 5 pA/pF. *Horizontal bars*, 200 msec. B, 293B-sensitive K^+ current obtained by digital subtraction in the absence (*left*; −IsK) and presence *(right*; +IsK) of IsK. *Vertical bars*, 4 pA/pF; *horizontal bars*, 200 (−IsK) and 500 (+IsK) msec. C, Current-voltage relationship for the 293B-sensitive current recorded in the cells shown in B. Same protocol as in legend to Fig. 1A.

additional experiments were performed to determine dose-effect relations at different membrane potentials in cells expressing KvLQT1 alone. The protocol consisted of depolarizing voltage steps, in 10-mV increments, applied to various voltages between −100 and +60 mV and followed by a step to −40 mV, where tail current amplitude was measured in the absence and presence of various concentrations of 293B. From the results of five different experiments, the calculated IC_{50} values were 15.6 μM at −20 mV, 10.1 μM at 0 mV, 7.2 μM at + 20 mV, and 7.1 μM at +40 mV.

The block produced by 293B on KvLQT1 current was not only voltage- but also time-dependent. The KvLQT1 current recorded during a depolarizing step to +40 mV in the presence of 293B was digitally subtracted from that recorded in control and then divided by the current recorded in control $[(i_{control} - i_{293})/i_{control}]$. This calculation gave the relative amount of block produced by 293B as a function of time during a depolarizing step. On the example shown in Fig. 3C, the block of KvLQT1 produced by 293B developed from 0% to a value of <30% within a 1-sec voltage step to +40 mV. In the absence of IsK, this curve was fitted by the sum of two exponential functions with time constants of 37.0 ± 6.8 and

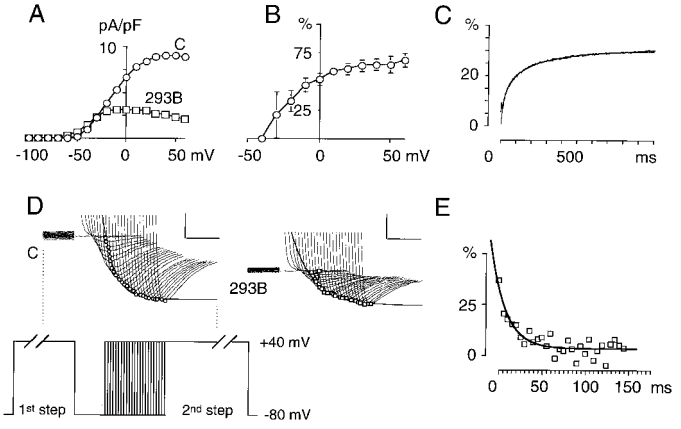

Fig. 3. Voltage- and time-dependence of the effects of 293B. A, KvLQT1 tail current-voltage relationship in control (C) and with 10 μM 293B. Data are averaged current tail amplitudes from four cells injected with KvLQT1 in the absence of IsK. The voltage potential was stepped to various voltages (prepulse potential) between −100 and +60 mV and then stepped back to −40 mV (pulse potential) where tail currents were measured. B, Voltage-dependence of 293B block at steady state. Same voltage protocol as in A. For each prepulse potential, the maximal tail current amplitude (measured using monoexponential fits forced to time 0) in the presence of 10 μM 293B was subtracted from that in control and divided by the maximal tail current amplitude in control. This value, which represents the percent of block produced by the drug at steady state, was plotted against the prepulse potential. Data are mean ± standard error from five different cells. C, Time-dependence for 293B block. The voltage protocol consisted of depolarizing steps from −80 to + 40 mV for 1 sec. The KvLQT1 current in the presence of 293B (10 μM) was digitally subtracted from that recorded in control and then divided by the current recorded in control [$(i_{control} - i_{293})/i_{control}$]. This calculation gave the relative amount of block (in percent) produced by 293B as a function of time during a depolarizing step. D, Current deactivation at −80 mV. *Bottom*, voltage protocol. Cells were depolarized from −80 to +40 mV for 1 sec and then clamped at −80 mV for increasing periods of time, in 5-msec increments, before a second depolarizing pulse was applied. For clarity, only the currents recorded during the second depolarizing pulse are superimposed in control (*left*) and with 293B (10 μM; *right*). Initial current amplitudes at the onset of the second depolarizing pulse (*open symbols*), which reflected deactivation kinetics, were fitted by a monoexponential function, as shown. The time constant was 18 msec in control and 34 msec with 293B. *Vertical bars*, 3 pA/pF; *horizontal bars*, 50 msec. Current amplitude at the end of the conditioning prepulse: 32 pA/pF in control and 22 pA/pF with 293B. E, Time dependence for 293B unblock. The value for $(i_{control} - i_{293})/i_{control}$ was calculated from the traces shown in D, plotted as percent against time, and fitted to a monoexponential (time constant, 17 msec). This relation reflects unblock kinetics.

324.3 ± 63.0 msec (six cells). In the presence of IsK, a single exponential with a time constant of 245.6 ± 19.0 msec correctly fitted the time-dependence of the block produced by 293B. The same approach was used to determine unblock kinetics on tail currents. On repolarization to −40 mV, current unblock occurred with much faster kinetics than current block during depolarization: current unblock was fitted by a monoexponential with a time constant of 13.1 ± 0.1 msec (five cells) in the absence of IsK and of 13.9 ± 0.8 msec in the presence of IsK. However, determination of drug unblock kinetics using tail currents was difficult because $i_{control}$ and i_{293} approximated 0 pA at the end of the pulse. With the aim to determine more reliably the unblock kinetics, another voltage protocol was used (Fig. 3D). Cells were depolarized from −80 to +40 mV for 1 sec and then maintained at the level of the holding potential for increasing periods of time before a second depolarizing pulse to +40 mV for 1 sec was applied. The initial current amplitude measured at the second depolarizing pulse reflected the degree of deactivation of the current at −80 mV. Cells stimulated with this protocol were recorded in control and in the presence of 293B. Then, $(i_{control} - i_{293})/i_{control}$ was calculated, plotted against time, and fitted to a monoexponential to appreciate unblock kinetics. Using this approach, unblock time constant was 17 msec on the example shown in Fig. 3E (i.e., significantly greater than the value determined with the current tail method). Taken together, these series of experiments suggest that 293B does not bind to the channel protein when the membrane potential is clamped at the holding potential (−80 mV) and binds only at depolarized voltages when KvLQT1 channels are in the open state. The kinetics for 293B to block KvLQT1 channels during depolarization are appreciably slower than the unblock kinetics on repolarization.

Using additional protocols as illustrated in Fig. 4, we found no evidence for use-dependence of the block. Fig. 4A shows an experiment performed in a cell sequentially depolarized at 0.2 Hz from −80 to +40 mV. In the first part of the experiment, the stimulation protocol was stopped for 30 sec, during which 293B was perfused. The voltage stimulation was started again for 40 sec and then stopped for 30 sec while the drug was washed off. In five different experiments, we observed that the amount of block produced by 293B under such conditions did not differ from that measured when the voltage stimulation was maintained. Finally, in four additional experiments, the drug was applied at a constant membrane potential of +40 mV. As shown in Fig. 4B, onset and offset kinetics of current block were not significantly affected by voltage stimulation.

293B blocks KvLQT1 current in cell-attached patches. In six additional experiments, KvLQT1 K^+ currents were recorded in the maxipatch cell-attached configuration (Fig. 5). When applied in the extracellular medium, 293B also blocked the time- and voltage-dependent K^+ current related to KvLQT1 cDNA expression, suggesting that 293B penetrates the cell to bind at a cytoplasmic site of the channel protein. In the cell-attached configuration, onset and offset kinetics of current block by 293B were in the same order as in whole-cell recordings.

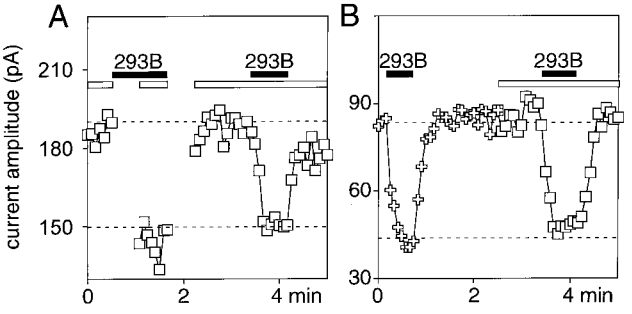

Fig. 4. Lack of use-dependence of the chromanol 293B effects. A and B, Outward current amplitude at +40 mV in a cell injected with 5 μg/ml KvLQT1 is plotted against time. 293B (10 μM) applied as indicated. A, Cell was sequentially depolarized at 0.2 Hz from −80 to +40 mV. In the first part of the experiment, voltage stimulation (*open horizontal bars*) was stopped for 30 sec, started again for 40 sec, and then stopped for 30 sec. In the second part of the experiment, the voltage stimulation was not interrupted. B, In the first part of the experiment (*crosses*), the membrane voltage was maintained at +40 mV. In the second part of the experiment, the cell was stimulated as in A but the cell was a different cell. *Open horizontal bars*, voltage stimulation.

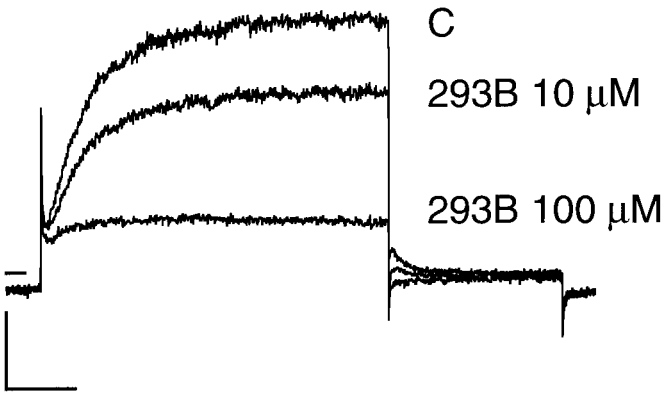

Fig. 5. Cell-attached maxipatch recordings in a COS-7 cell injected with 50 μg/ml pCI-KvLQT1 plus 50 μg/ml pCR−IsK. Superimposed current traces recorded in control (C) and in the presence of 10 μM and 100 μM 293B applied in the extracellular medium. The potential was stepped from −80 to +40 mV and then back to −40 mV. Potentials are expressed relative to the bath. The cell membrane potential considered as 0 mV when bathed in the high K^+ extracellular medium. *Vertical bar*, 100 pA; *horizontal bar*, 200 msec.

Cromakalim blocks KvLQT1 K^+ current. Finally, we explored the effects on KvLQT1 currents of cromakalim [*trans*-6-cyano-3-hydroxy-2,2-dimethyl-4-(2-oxo-1-pyrrolidinyl)-chromane], another chromanol derivative. The main property of cromakalim is to act as a K^+ channel opener targeted to ATP-sensitive K^+ channels (15). However, in a previous study conducted in guinea-pig ventricular myocytes (16), we observed that potassium channel openers not only activate a time-independent current corresponding to the ATP-sensitive K^+ current but also suppress outward tail currents triggered by cell repolarization. Our findings with 293B prompted us to search for an effect of cromakalim on recombinant KvLQT1 current. As illustrated in Fig. 6, we found that cromakalim, like 293B, also acted as a KvLQT1 current blocker. On average, cromakalim, when used at 10 μM (the concentration used to activate ATP-sensitive K^+ channels in cardiac myocytes), blocked 30 ± 6% of the tail current amplitude related to KvLQT1 expression in COS-7 cells.

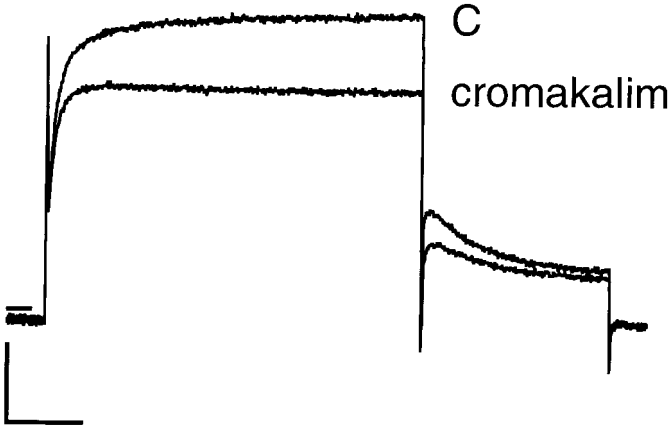

Fig. 6. The effects of cromakalim on the KvLQT1-related current. Superimposed current traces recorded in control (C) and in the presence of cromakalim (10 μM) in a COS-7 cell injected with 5 μg/ml pCI-KvLQT1 without IsK. The protocol consisted of depolarizing voltage steps applied from −80 to +40 mV and then back to −40 mV. *Vertical bar*, 2 pA/pF; *horizontal bar*, 200 msec.

Discussion

Our results show that (i) the chromanol 293B binds directly to KvLQT1 channel protein but not to the IsK channel regulator, (ii) expression of IsK does not modify 293B affinity for KvLQT1 channels, and (iii) 293B exerts strong voltage- and time-dependent-blocking effects on KvLQT1 channels. This pharmacological profile is consistent with an open-channel block. Another possible explanation is that 293B binds at some site on the channel protein with accessibility that is state-dependent. The kinetics for 293B to associate with its binding site during depolarization is not instantaneous but takes a few tenths of a msec in the absence of IsK and a few hundredths of a msec in the presence of IsK. In contrast, unbinding of the drug to its receptor as induced by repolarization is fast and ~5–10-fold faster than deactivation kinetics of the current. The lack of use-dependence of the effects of 293B is not surprising in regard to the very rapid unblock kinetics of the drug. Finally, we show that another chromanol compound, cromakalim, which is well known for its K^+ channel-activating properties targeted to ATP-sensitive K^+ channels, also exerts measurable KvLQT1 blocking effects at concentrations compatible with its K^+ channel-activating properties in cardiac muscle.

Earlier reports concerning the chromanol compound 293B have demonstrated the ability of this drug to block a cAMP-activated K^+ conductance in colonic cells (18, 19). Subsequently, it was shown that 293B blocked a time-dependent K^+ conductance in *X. laevis* oocytes injected with IsK cRNA (12) with an IC_{50} value of 6.7 μM (i.e., close to the value for 293B to block KvLQT1 current in the current report). In contrast, the drug was ineffective on the K^+ current related to *Kir2.1* or *Kv1.1* expressions (12). Most recently, however, it was shown that IsK expression in *X. laevis* oocytes does not create recombinant K^+ channel proteins *per se* but instead reveals an endogenous K^+ channel with strong homologies with the *KvLQT1* gene product identified in the human heart (5). On the basis of experiments performed previously in *X. laevis* oocytes, it thus remained obscure whether 293B binds to the IsK regulator or to the KvLQT1 channel protein itself. Our work addresses this important question because it demonstrates that the affinity for 293B to block KvLQT1 current is independent of the presence of IsK. The *KvLQT1* gene is expressed not only in the heart but also in numerous other organs, including the kidney, pancreas, adrenal and salivary glands, and stomach (for a more complete list, see Ref. 17). Depending on the tissue, the IsK regulator should or should not be coexpressed together with KvLQT1. Our results demonstrate that 293B is a valuable tool with which to explore the role of KvLQT1 channels in a tissue regardless of the presence of IsK.

This assumption is caricatural as far as the heart muscle is concerned. Class III antiarrhythmic agents of the Vaughan-Williams classification, which is based on the effects of drugs on the morphology of the cardiac action potential (20), prolong the plateau duration and thus prolong refractoriness. The simplest way to achieve this goal is to block myocardial K^+ channels because less net outward current will be available to repolarize the cells. Virtually all members of pure class III antiarrhythmic drugs retain voltage-dependent K^+ channel block as their mechanism of action (21); more precisely, these drugs usually block the rapid component of the

delayed rectifier termed i_{Kr} (11), as is the case with D-sotalol, dofetilide, sematilide, risotilide, E4031, and almokalant. At the molecular level, the i_{Kr} current is conducted through the HERG channel protein (22), which is encoded by a gene located on chromosome 7q35–36 and is responsible for the congenital long QT 2 phenotype (23). In opposition to class I antiarrhythmic drugs, class III agents targeted to HERG have an unfavorable frequency-dependent profile (so-called reverse frequency dependence) because they are more active at slow than at fast rates (24). Theoretically, this may limit their activity during tachycardia and produce excessive prolongation when the cardiac rate is slow, leading to torsades de pointe arrhythmias. Thus, novel class III antiarrhythmic drugs lacking an unfavorable frequency-dependent profile and therefore not targeted to HERG are needed. During an action potential, the i_{Ks} current slowly activates and participates to cell repolarization in concert with i_{Kr} and other K^+ currents. Repolarization in turn switches off the i_{Ks} current through deactivation mechanisms. Because deactivation is slow during diastole, at high frequencies deactivation is incomplete before the next action potential arises, leading i_{Ks} channels to remain permanently in the open state (25). Thus, KvLQT1 channels, which are expressed at a high level in the heart together with the IsK regulator (4, 5, 17), may represent a molecular target for novel class III antiarrhythmic agents with a more favorable rate-dependent profile. The pharmacological profile for 293B as reported here makes this drug a valuable tool for investigation of the antiarrhythmic properties of an i_{Ks} blocker. It can be anticipated that at a slow heart rate, the effect of the drug on the cardiac action potential should be modest because (i) i_{Ks} activation kinetics are slow in relation with the duration of the action potential, (ii) 293B binding kinetics on opened i_{Ks} channels also are slow, and (iii) 293B unbinding kinetics are fast and much faster than deactivation kinetics leading i_{Ks} tail current available for terminal phase 3 repolarization. At high rates of stimulation, the effect of the drug on action potential duration should be more pronounced because a significant proportion of i_{Ks} channels are permanently opened. As yet, little information is available as to whether 293B is specific for KvLQT1 K^+ channels in cardiac cells. Busch et al. (26) suggested recently that in the guinea-pig heart, 293B exerts no significant effects on the rapid component of the delayed rectifier i_{Kr}, on the inwardly rectifying instantaneous K^+ current or the L-type Ca^{2+} current (26). Regardless of the specificity of 293B for KvLQT1 in the heart muscle, KvLQT1 channels are widely distributed in the organism and KvLQT1 blocking drugs that should be developed in the context of arrhythmias are suspected to have side effects that would result from their action on KvLQT1 channels in other tissues.

Acknowledgments

We thank Béatrice Leray and Marie-Joseph Loirat for expert technical assistance with cell cultures and plasmid amplifications.

References

1. Roden, D. M., R. Lazzara, M. Rosen, P. J. Schwartz, J. Towbin, and G. M. Vincent. Multiple mechanisms in the long-QT syndrome. *Circulation* **94:** 1996–2012 (1996).
2. Neyroud, N., F. Tesson, I. Denjoy, M. Leibovici, C. Donger, J. Barhanin, S. Fauré, F. Gary, P. Coumel, C. Petit, K. Schwartz, and P. Guicheney. A novel mutation in the K^+ channel KvLQT1 causes the Jervell and Lange-Nielsen cardioauditory syndrome. *Nat. Genet.* **15:**186–189 (1997).
3. Lee, M. P., R. J. Hu, L. A. Johnson, and A. P. Feinberg. Human KvLQT1 gene shows tissue-specific imprinting and encompasses Beckwith-Wiedemann syndrome chromosomal rearrangements. *Nat. Genet.* **15:**181–185 (1997).
4. Barhanin, J., F. Lesage, E. Guillemare, M. Fink, M. Lazdunski, and G. Romey. KvLQT1 and IsK (minK) proteins associate to form the I_{KS} cardiac potassium current. *Nature (Lond.)* **384:**78–80 (1996).
5. Sanguinetti, M. C., M. E. Curran, P. S. Spector, A. Zou, J. Shen, D. Atkinson, and M. T. Keating. Coassembly of KvLQT1 and minK (IsK) to form cardiac I_{KS} potassium channel. *Nature (Lond.)* **384:**80–83 (1996).
6. Goldstein, S. A. N., and C. Miller. Site-specific mutations in a minimal voltage-dependent K^+ channel alter ion selectivity and open-channel block. *Neuron* **7:**403–408 (1991).
7. Takumi T., H. Ohkubo, and S. Nakanishi. Cloning of a membrane protein that induces a slow voltage-gated potassium current. *Science (Washington D. C.)* **242:**1042–1045 (1988).
8. Tzounopoulos T., H. R. Guy, S. Durell, J. P. Adelman, and J. Maylie. MinK channels form by assembly of at least 14 subunits. *Proc. Natl. Acad. Sci. USA* **92:**9593–9597 (1995).
9. Attali B., E. Guillemare, F. Lesage, E. Honoré, G. Romey, M. Lazdunski, and J. Barhanin. The protein IsK is a dual activator of K^+ and Cl^- channels. *Nature (Lond.)* **365:**850–852 (1993).
10. Lesage, F., B. Attali, J. Lakey, E. Honoré, G. Romey, E. Faurobert, M. Lazdunski, and J. Barhanin. Are *Xenopus* oocytes unique in displaying functional IsK channel heterologous expression? *Recept. Channels* **1:**143–152 (1993).
11. Sanguinetti, M. C., and N. K. Jurkiewics. Two components of cardiac delayed rectifier K^+ current: differential sensitivity to block by class III antiarrhythmic agents. *J. Gen. Physiol.* **96:**195–215 (1990).
12. Suessbrich, H., M. Bleich, D. Ecke, M. Rizzo, S. Waldegger, F. Lang, I. Szabo, H. J. Lang, K. Kunzelmann, R. Greger, and A. E. Busch. Specific blockade of slowly activating I_{sK} channels by chromanols: impact on the role of I_{sK} channels in epithelia. *FEBS letters 396:*271–285 (1996).
13. Mohammad-Panah, R., S. Demolombe, D. Riochet, G. Loussouarn, V. Leblais, I. Baró, and D. Escande. Hyperexpression of recombinant CFTR in heterologous cells alters its physiological properties. *Am. J. Physiol*., in press.
14. Romey, G., B. Attali, C. Chouabe, I. Abitbol, E. Guillemare, J. Barhanin, and M. Lazdunski. Molecular mechanism and functional significance of the MinK control of the KvLQT1 channel activity. *J. Biol. Chem.* **272:** 16713–16716 (1997).
15. Escande, D., D. Thuringer, S. Le Guern, and I. Cavero. The potassium channel opener cromakalim (BRL 34915) activates ATP-dependent K^+ channels in isolated cardiac myocytes. *Biochem. Biophys. Res. Commun.* **154:**620–625 (1988).
16. Escande, D., D. Thuringer, S. Le Guern, J. Courteix, M. Laville, and I. Cavero. Potassium channel openers act through an activation of ATP-sensitive K^+ channels in guinea-pig cardiac myocytes. *Pflueg. Arch. Eur. J. Physiol.* **414:**669–675 (1989).
17. Yang, W. P., P. C. Levesque, W. A. Little, M. Lee Conder, F. Y. Shalaby, and M. A. Blanar. KVLQT1, a voltage-gated potassium channel responsible for human cardiac arrhythmias. *Proc. Natl. Acad. Sci. USA* **94:**4017–4021 (1997).
18. Lohrmann E., I. Burhoff, R. B. Nitschke, H. J. Lang, D. Mania, H. C. Englert, M. Hropot, R. Warth, W. Rohm, M. Bleich, and R. A. Greger. New class of inhibitors of cAMP-mediated Cl^- secretion in rabbit colon, acting by the reduction of cAMP-activated K^+ conductance. *Pflueg. Arch. Eur. J. Physiol.* **429:**517–530 (1995).
19. Warth R., N. Riedemann, M. Bleich, W. Van Driessche, A. E. Busch, and R. Greger. The cAMP-regulated and 293B-inhibited K^+ conductance of rat colonic crypt base cells. *Pflueg. Arch. Eur. J. Physiol.* **432:**81–88 (1996).
20. Vaughan-Williams E. M. A classification of antiarrhythmic actions reassessed after a decade of new drugs. *J. Clin. Pharmacol.* **24:**129–147 (1984).
21. Spector P. S., M. E. Curran, M. T. Keating, and M. C. Sanguinetti. Class III antiarrhythmic drugs block HERG, a human cardiac delayed rectifier K^+ channel. *Circ. Res.* **78:**499–503 (1996).
22. Sanguinetti M. C., C. Jiang, M. E. Curran, and M. T. Keating. A mechanistic link between an inherited and an acquired cardiac arrhythmia: HERG encodes the I_{Kr} potassium channel. *Cell* **81:**299–307 (1995).
23. Sanguinetti M. C., M. E. Curran, P. S. Spector, and M. T. Keating. Spectrum of HERG K^+ dysfunction in a inherited cardiac arrhythmia. *Proc. Natl. Acad. Sci. USA* **93:**2208–2212 (1995).
24. Roden D. M. Current status of class III antiarrhythmic drug therapy. *Am. J. Cardiol.* **72:**44B–49B (1993).
25. Jurkiewicz N. K., and M. C. Sanguinetti. Rate-dependent prolongation of cardiac action potentials by a methanesulfonanilide class III antiarrhythmic agent: specific block of rapidly activating delayed rectifier K^+ current by dofetilide. *Circ. Res.* **72:**75–83 (1993).
26. Busch A. E., H. Suessbrich, S. Waldegger, E. Sailer, R. Greger, H. J. Lang, F. Lang, K. J. Gibson, and J. G. Maylie. Inhibition of i_{KS} in guinea-pig cardiac myocytes and guinea-pig IsK channels by the chromanol 293B. *Biophysl J.* **72:**2 A50 (1997).

Send reprint requests to: Professor Denis Escande, Lab de Physiopathologie et de Pharmacologie Cellulaires et Moléculaires, INSERM CJF 96.01, Bât HNB, Hôpital Hotel-Dieu, BP 1005, 44093 Nantes, France. E-mail: denis.escande@sante.univ-nantes.fr